CCFE-PR(15)119

A. Boboc, B.Bieg, R.Felton, S.Dalley and Yu. Kravtsov

A novel calibration method for the JET Real-Time Far Infrared Polarimeter and integration of polarimetry-based line-integrated density measurements for machine protection of a fusion plant

A novel calibration method for the JET Real-Time Far Infrared Polarimeter and integration of polarimetry-based line-integrated density measurements for machine protection of a fusion plant

A. Boboc[1], B.Bieg[2], R.Felton[1], S.Dalley[1] and Yu. Kravtsov[2]

[1] CCFE, Culham Science Centre, Abingdon, OX14 3DB, UK
[2] Maritime University of Szczecin, Institute of Physics, Szczecin, Poland

A novel calibration method for the JET Real-Time Far Infrared Polarimeter and integration of polarimetry-based line-integrated density measurements for machine protection of a fusion plant

A. Boboc[1,a)] , B.Bieg[2], R.Felton[1], S.Dalley[1] and Yu. Kravtsov[2]

EUROfusion Consortium, JET, Culham Science Centre, Abingdon, OX14 3DB, UK
[1] *CCFE, Culham Science Centre, Abingdon, OX14 3DB, UK*
[2] *Maritime University of Szczecin, Institute of Physics, Szczecin, Poland*
[a)] Corresponding author e-mail: Alexandru.Boboc@ccfe.ac.uk

The JET Far-Infrared (FIR) interferometer/polarimeter diagnostic is a laser-based instrument used for measuring several plasma parameters: electron line-integrated density via interferometry and Faraday rotation and Cotton Mouton angle via polarimetry. Since early 2000 there were many developments of this instrument to increase the reliability and enhance the measurement capabilities. The latest ones, presented in this paper, are a new calibration and a complex self-validation mechanism for the real-time polarimeter based on the Complex Amplitude Ratio Technique and integration of the polarimetry measurements into the JET plasma density control (gas feedback control) and machine protection systems (Neutral Beam Injection heating safety interlocks).

Introduction

The JET polarimeter[1,2,3,4,5,6] is more than 20 years old. To date, its use has been limited to a narrow area of experiments such as q-profile control or Motional Stark Effect diagnostic calibration. Recent developments on reconstruction of JET magnetic equilibria require measurements of Faraday rotation angle together with an automatic way to validate the data and with a time resolution in millisecond range. This was not possible to do with the original CAMAC-based infrastructure and since 2011 developments of the polarimeter have been focused on upgrading the real-time infrastructure based on the PowerPC architecture.

The installation of JET's ITER-like wall has caused new types of diagnostic issues such as tungsten impurity influxes during plasma pulses that heavily affect FIR interferometry (signal loss for up to half second) but also other systems as well. At that stage it became critical to assess if the line-integrated density measurements from polarimetry could be used for density control and machine protection even if the data quality and the error level was not the same as the one provided by the interferometer.

After a few years of development and testing during recent campaigns we have implemented a new real-time calibration of polarimetry to output not only the Faraday rotation angle measurements but also measurements of line integrated density and advanced validation flags in real-time.

The paper is organised as follows: section I contains a detailed description of the JET polarimeter including hardware, software as well as calibration process; section II is dedicated to the method of Complex Amplitude Ratio[8] and evaluation of line-integrated measurements from polarimetry. Various measurements are analysed and discussed in section III and the way these were integrated within JET machine protection Systems and Machine protection is explained in section IV. The remainder of the paper is dedicated to the conclusion and proposed further developments.

I. JET REAL-TIME POLARIMETER

A. General description

The JET FIR diagnostics rely on using two types of far infrared lasers (Terahertz region in frequency domain) with wavelengths of 195μm (Deuterated cyanide(DCN) laser) and 119μm (Methanol laser) as at these wavelengths the high temperature plasmas are optically transparent. The current diagnostic configuration probes the plasma via eight channels, four vertical and four lateral, with a sensitivity of $3x10^{17}$particle/m^2 for the line-integrated density and 0.05-0.2 degrees for the Faraday rotation angle measurements. The polarimetry side is implemented by using only the DCN laser as at this wavelength the expected Faraday rotation angle is large (up to 70 degrees).

The diagnostic system consists of components located in three different major areas: laboratory, basement and torus area as shown in figure 1.

All the three areas are purged 24h/day with very dry air at -60 degrees Dewpoint humidity level to minimise FIR beam losses by absorption.

The laboratory area contains the lasers with ancillary equipment; optical tables made of solid granite, cryogenic liquid helium cooled detectors systems and electronics used for processing of the measurements.

The basement area consists of a large box 25 meters long and cross section of about 1.5 by 2 meters attached to the ceiling covering the space from the lab area to the bottom of the diagnostic tower located in the torus hall.

The torus hall area contains mainly the diagnostic tower. This is a 14 meter high, 50 ton air-tight structure containing the input optics and recombination plates as well as the motorised half-wave plate (HWP) and associated opto-mechanical assemblies for the polarimetry calibration.

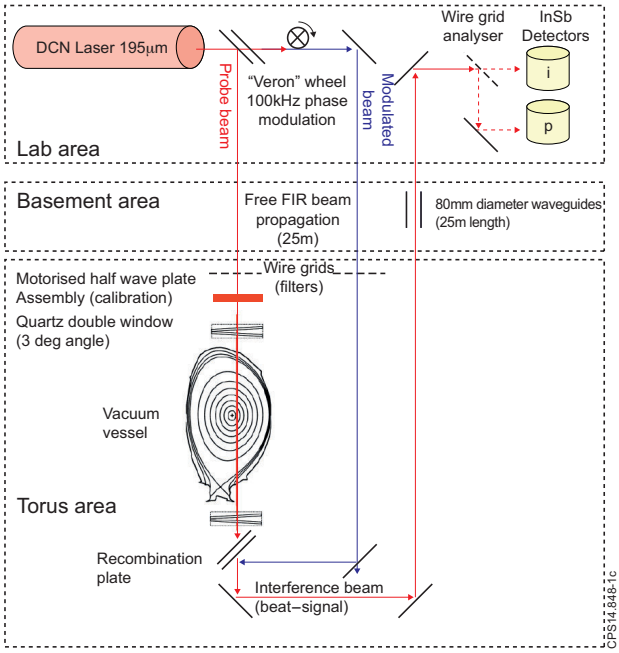

Figure 1: Schematic representation of the JET FIR diagnostic system as used by the polarimeter

Nearly all the optics can be moved remotely using pneumatic motors with the exception of the half-wave plate plates that are driven by standard electrical stepper motors.

The three areas are separated by 90μm Polymethylpentene (TPX) pellicle windows that have the role of keeping the enclosures sealed but that act also as a safety barrier (critical during tritium experiments). These are also required to support the depression in the torus hall, a safety feature (nominally in the range of 200 to 250 Pascal; more than 500 Pa during Deuterium-Tritium (D-T) campaign).

In terms of optical principle, the operation of the instrument is as follows: a linearly polarised laser beam is emitted by the DCN laser system. This is split in two components, one so-called probe signal that passes through the plasma and another one that is phase modulated with a Doppler wheel at a frequency of 100 kHz. After passing through the plasma, the probe beam becomes elliptically polarised with its polarisation plane rotated due to the Cotton-Mouton and Faraday effects, respectively with respect the initial polarisation state. The two beams (probe and modulated) are recombined at the recombination plate and the resulting interference beat-signal returns back to the laboratory where is detected by the InSb cryogenic detectors (cooled at liquid helium temperature). From there the signals are processed by the data acquisition system.

For each line of sight or channel, due to losses, the level of power that reaches the detectors is a few microwatts even if the original laser power is of the order of tens of milliwatt.

B. Short history

The polarimeter was originally designed in 1987 mainly for Faraday angle measurements. In 2001, new electronics were commissioned based on a real-time PowerPC VME technology for calculations of Faraday angle and q-profile for real-time control of the plasma[11] together with the implementation of real-time calibration on the CAMAC system using novel half-wave plate rotators based on stepper motors (magnetically shielded) and remotely controlled by FPGA-based cards. All the parameters are set remotely via software controlled by the JET Control and Data Acquisition System (CODAS).

At a later stage (2004), the system was optimised to measure also the Cotton-Mouton[1] phase shift. In preparation for the 2008-2009 experimental campaigns there was a requirement to set-up the polarimeter for ITER-relevant high current plasma experiments (4.5-5MA) and high density (90% of Greenwald limit). This is equivalent to a requirement to keep the error level below 0.2 degrees for values of Faraday rotation angle of 70-80 degrees. This was at the limit of the existing electronics and the ADCs were upgraded to 16bits ADC for the real-time system.

In 2013 a novel calibration method based on Complex Amplitude Ratio was implemented and tested extensively on a selection of 700 pulses covering 10 years of operation of the polarimeter system. A code written in Python was developed for automatic generation of the offline Processed Pulse Files (PPFs) including automatic validation and integration with the reconstruction program EFIT++[12] recently deployed at JET. More recently, in September 2014, the real-time integration into the JET safety-system was completed, in particular with the Plasma Density Validation System (PDV) that provides the density measurements for plasma gas injection feedback and control as well as the Neutral Beam Injection safety interlocks.

C. Hardware description

Most implementations of polarimeters are for measuring Faraday rotation angle alone and therefore provide a calibration for this measurement. The most common way to implement this type of calibration is to use a half-wave plate (HWP). This optical component rotates the polarisation plane corresponding to twice the angle between the optical axis and the input polarisation plane of a laser beam that traverses it. By comparing the mechanical rotation of the HWP with the detected laser signals one can obtain the calibration curve for the actual Faraday rotation measurements in angular units.

The JET polarimeter uses this technique[3] and the main points of this are described schematically in the figure 2. The main part of the calibration hardware is the half-wave plate rotator assembly that contains a wire grid used for optical filtering (it ensures the beam entering plasma is linearly polarised) a half-wave plate, a stepper motor and a potentiometer linked with a high quality gearbox. All these components are installed on a fibreglass frame and fixed to the diagnostic tower. The assemblies are very close to the JET mechanical structure (50 to 100cm depending on channel).

Communication to the half-wave plate assemblies is done via serial link and I/O from a CODAS CAMAC system that also is used for setting up and monitoring. Prior to a pulse the diagnostic operator sets up the calibration range of the instrument. These settings are sent via software to the motor controller that will move automatically the half-wave plate for the desired calibration range as well as returning back to the neutral position. In the current setup, this corresponds with a beam polarisation of 45degrees for the vertical channels to maximise Cotton-Mouton

measurements[3] and 0 degrees for lateral channels relative to the toroidal field direction.

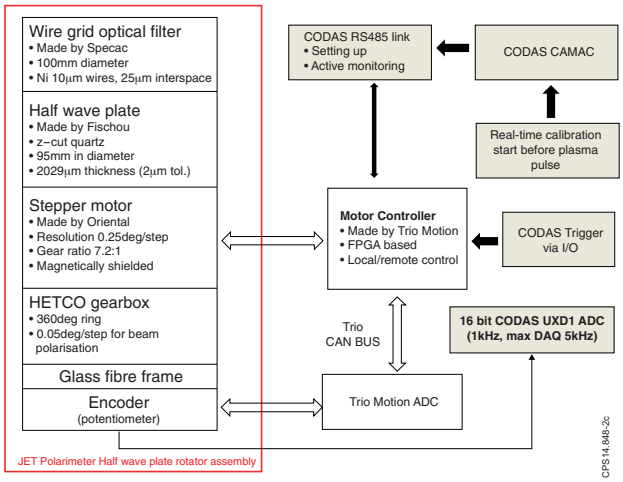

Figure 2. The CAMAC-based JET polarimeter implementation

D. PowerPC Hardware

The real-time VME is based on PowerPC architecture and was developed in 2001 and upgraded over the years to have the final form as schematically represented in figure 3. The most recent change was the operating system and the compiler on the master PPC as the new calibration software required implementation of new libraries able to deal with trigonometry functions on complex numbers, not normally provided for in the real-time PowerPC architecture.

The analogue signals are currently acquired by ADC modules developed in-house by Control and Data Acquisition System(CODAS). The system is synchronised with JET Composite Timing and Trigger System (CTTS) and controlled remotely by daemon software that runs on a Solaris work station and via a dedicated Graphical User Interface (GUI) for setting up various parameters. Data acquisition is integrated within the JET Pulse File (JPF) database every pulse.

The real-time FIR interferometer/polarimeter signals are output to the JET Real-Time Data Network (RTDN) via Asynchronous Transfer Mode (ATM) protocol.

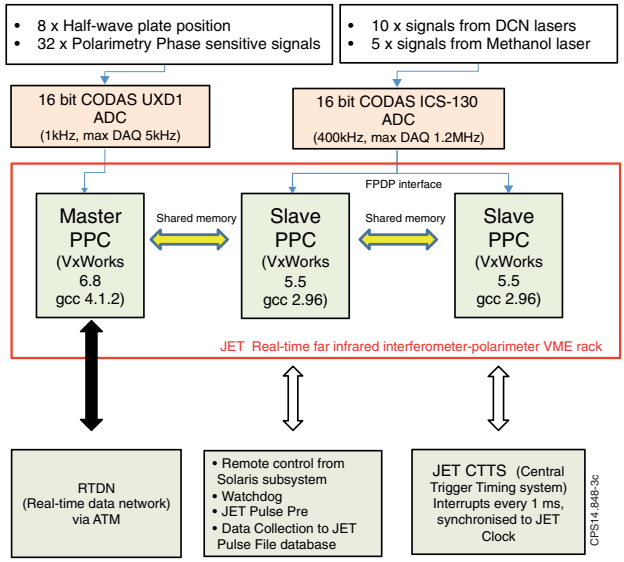

Figure 3. JET Far Infrared (FIR) Real-time interferometer-polarimeter implementation

E. Calibration logic

The automatic half-wave plate rotation required for an online calibration procedure was installed in 2002 but only recently was an algorithm implemented for real-time data analysis using the Complex Amplitude Ratio (CAR) method. This is described in the section II.

The time-flow of the calibration is depicted in figure 4 and can be explained in a simplified form as follows: two minutes and a half before the pulse the valve that feeds the DCN laser with Deutherated Methane (CD_4) is activated and the parameters corresponding to the calibration range for the polarimeter are sent to the motor controller. The calibration, with cycle of 10s, starts when a trigger is sent to the controller when data collection is active. After that there are 5 seconds in which the calibration has to run for all channels after which the results can be applied in real-time to the input signals. During the actual plasma pulse (after 40 seconds) the calibration is applied and data is calculated and evaluated on every 1 ms cycle and published via RTDN as shown in Figure 4.

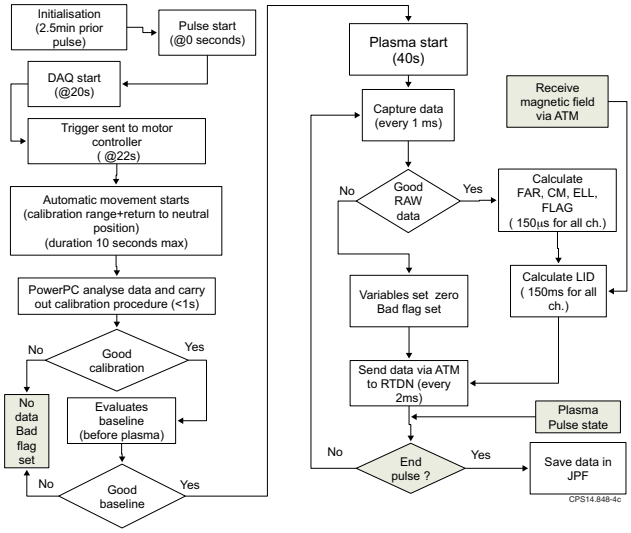

Figure 4: Calibration procedure for one channel of JET polarimeter

More detailed information is displayed in figure 5 where the raw data measured by the analogue phase-sensitive electronics during the process of calibration alone (see section III for definition of raw data) as well as the output of measurements for a JET pulse are pictured. In this particular example the data is displayed from channel 3 that was set to cover a Faraday rotation angle range of 30 degrees from an initial position of 45degrees. At 22 seconds in the pulse a trigger is sent to the motor controller, this automatically rotates the plate for the desired range (in this case 15 degree mechanical rotation of the HWP that corresponds to 30 degrees of laser beam polarisation) and returns it to the neutral position of 45 degrees. The system was designed to cover up to 90 degrees of polarisation scan plus return to the neutral position scan in 10 seconds maximum.

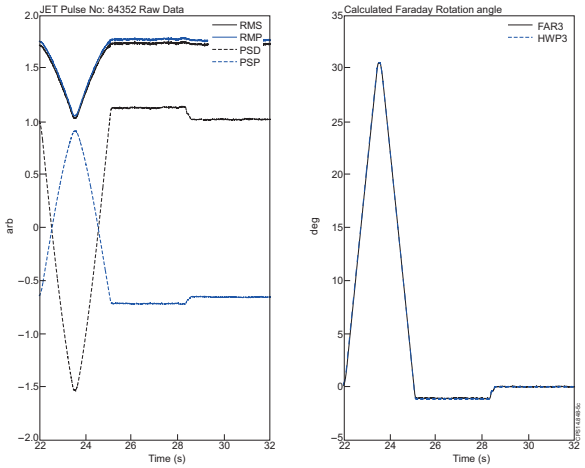

Figure 5:Real-time raw signals (left side) and calculated Faraday angle (FAR3) compared with mechanical HWP position (HWP3) in degrees for channel 3.

II. Complex Amplitude Ratio (CAR) method

A. Basic physics considerations

The principles of interferometry/polarimetry have been described in detail in several references[1,2]. Interpretation of the measurements from this type of device must take into account several properties of the plasma: refractive index, optical activity and birefringence. Due to these three effects, linearly polarised electromagnetic radiation sent into a plasma can provide three measurements:

- *Interferometry phase shift* of the probe beam proportional to the plasma electron line-integrated density (LID)
- *Faraday rotation angle (FAR)* of the polarisation plane that contains information about the magnetic field component in the direction of propagation of the beam and thus allowing obtaining information about the radial profile of the current flowing in the plasma
- *Cotton-Mouton (CM) phase shift angle* between the two orthogonal components of the electric vector as the FIR beam becomes elliptically polarised. These measurements can be also used to recover LID.

In the first approximation, one can write these measurements in mathematical form as follows:

Interferometry phase shift

$$\varphi_{\mathrm{int}erf} \propto \frac{1}{\lambda}\int n_e \; dz \tag{1}$$

Faraday rotation Angle

$$\Delta\Psi = \Psi - \Psi_0 \propto \lambda^2 \int n_e \; B_z \; dz \tag{2}$$

Cotton-Mouton angle

$$\Phi = \varphi - \varphi_0 \propto \lambda^3 \int n_e \left(B_x^2 - B_y^2\right) dz \tag{3}$$

Here z is the propagation direction of the laser beam, λ is the laser wavelength, n_e is the electron plasma density; B_x, B_v and B_z and are the components of the magnetic field; Ψ_0 and φ_0 are the initial azimuth angle and phase shift; Ψ and φ are the measured azimuth angle and phase shift during plasma at a certain time point.

B. Preamble

An optical system such as the JET FIR system contains many components such as lenses, mirrors, beam-splitters, windows, polarisers, phase retarders, isotropic and dichroic attenuators. The previous calibration method, based on the Stokes vector technique[7] and the Müller matrix formalism[6], have the following limitations

- Many assumptions about the system
- Range of parameters limited (not very high Faraday or CM angle for example)

- Complicated mathematics and fitting procedures
- Not suitable for real-time where execution times have to be 100μs and also due to other input parameters required not being available in real-time

The Complex Amplitude Ratio[9] on the other hand is a novel technique whose methodology reduces to determination of three complex numbers by simple inversion of transfer matrix, is fast and therefore suitable for real-time applications. The limitations to its application are mainly technical as it involves the use of complex numbers and normally real-time architectures do not come by default with packages that can perform such calculations. In addition, it must be possible to represent all polarising components in the system by a 2x2 Jones matrix (see below).

C. Polarization state description

The polarisation state of an elliptically polarised and rotated wave is schematically described in figure 6. The electrical vector can be considered as a complex phasor as follows:

a) complex electrical vector $\mathbf{E}$:

$$\mathbf{E} = E_x \mathbf{i} + E_y \mathbf{j} = E_{0x} e^{i\varphi_x} \mathbf{i} + E_{0y} e^{i\varphi_y} \mathbf{j} \quad (4)$$

b) angular variables (Θ, φ):

- the auxiliary angle Θ – the ratio between the amplitudes of orthogonal components of the electrical vector:

$$\tan\Theta = \frac{|E_y|}{|E_x|} = \frac{E_{0y}}{E_{0x}} \quad (5)$$

- the phase shift difference φ – the phase difference between two orthogonal components of the electrical vector:

$$\varphi = \varphi_y - \varphi_x \quad (6)$$

Note: many books use α as an amplitude ratio angle and δ as a phase difference; here we are using the convention from previous JET papers[3]: (Θ, φ).

c) complex amplitude ratio (CAR) defined as:

$$\zeta = \frac{E_y}{E_x} = \tan\Theta \exp(i\varphi) \quad (7)$$

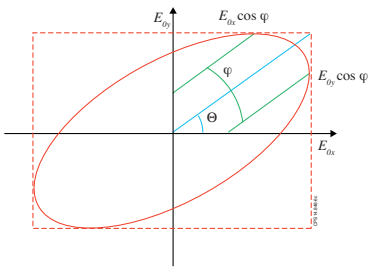

Figure 6: Polarisation state diagram

D. Initial polarisation state

The calibration scan contains three elements: the neutral position that is the position prior to the plasma pulse and the upper and lower limits corresponding to the expected Faraday Rotation angle for that particular channel during a particular plasma experiment.

The initial polarisation state is linear $(\varphi_0 = 0)$, set by the half-wave plate $(\Theta_0 = HWP)$.

Therefore the initial complex amplitude ratio can be calculated as:

$$\zeta_0 = \tan(HWP) \quad (8)$$

E. Signal detection

At JET, for each line of sight or channel, a polarisation analyser (wire grid) separates the two orthogonal components of the polarisation that are acquired by the interferometer and polarimetry detectors, called $i(t)$ and $p(t)$ respectively.

After analogue filtering and amplification, these signals are processed via analogue phase sensitive electronics to obtain four measurements as in the equation[6]:

$$RMS = < i \times i > \quad RMP = < i^* \times i^* >$$
$$PSD = < i \times p > \quad PSP = < i^* \times p > \quad (9)$$

Where i^* is i shifted by 90 deg.

These four signals can be represented as signal ratios called R and R' which are related to the polarisation (Θ, φ) of the detected beam:

$$\begin{cases} R = \dfrac{PSD}{RMS} = K^{-1}\tan(\Theta)\cos(\varphi) \\ R' = \dfrac{PSP}{\sqrt{RMS \cdot RMP}} = K^{-1}\tan(\Theta)\sin(\varphi) \end{cases} \quad (10)$$

where K is a calibration factor introduced by electronic system.

This final, measured polarisation state can be expressed as the Complex Amplitude Ratio (CAR) as follows:

$$\zeta_m = (R + iR') = K^{-1}\zeta_d \quad (11)$$

where ζ_d is the polarisation state of the beam at the detector system.

F. Calibration method

In the absence of the plasma, the initial polarisation state is changed between HWP and detectors by various optical components (lenses, mirrors, plates, beam splitters, wave guides), acting as polarizers, phase retarders, isotropic and dichroic attenuators. In our proposal we assume that optical properties of such a system can be modelled by Jones matrix formalism[9]:

$$\mathbf{J}^{op} = \begin{bmatrix} j_{11} & j_{12} \\ j_{21} & j_{22} \end{bmatrix} \quad (12)$$

The beam with initial polarisation $\mathbf{E}_0$ or ζ_0 set by the half-wave plate, has a final polarisation given by the electric vector $\mathbf{E}_d = \mathbf{J}^{op}\mathbf{E}_0$ or the complex amplitude ratio

$$\zeta_d = \frac{E_{dy}}{E_{dx}} = \frac{j_{21}E_{0x} + j_{22}E_{0y}}{j_{11}E_{0x} + j_{12}E_{0y}} = \frac{1 + \frac{j_{22}}{j_{21}}\frac{E_{0y}}{E_{0x}}}{\frac{j_{11}}{j_{21}} + \frac{j_{12}}{j_{21}}\frac{E_{0y}}{E_{0x}}}$$

or (13)

$$\zeta_d = \frac{1 + a\zeta_0}{b + c\zeta_0}$$

The final, measured polarisation state will be:

$$\zeta_m = K^{-1}\zeta_d = \frac{1 + A\zeta_0}{B + C\zeta_0} \qquad (14)$$

where $A = a$, $B = b \cdot K$, $C = c \cdot K$

The full characteristics of the optical and electronic systems can then be calculated in the calibration process using these three complex parameters *A*, *B* and *C*.
These parameters, can be determined from the measurements for arbitrary initial polarisation (*k*), described by complex amplitude ratio ζ_{0k} , $k = 1,2,3$:

$$\zeta_{mk} = \frac{1 + A\zeta_{0k}}{B + C\zeta_{0k}}$$

Hence (15)

$$B\,\zeta_{mk} + C\zeta_{0k}\,\zeta_{mk} - A\zeta_{0k} = 1$$

This relation can be transformed into a system of three linear equations for three complex parameters A , B and C :

$$\mathbf{M} \cdot \mathbf{X} = \mathbf{1}$$

where

$$\mathbf{M} = \begin{bmatrix} -\zeta_{01} & \zeta_{m1} & \zeta_{01}\zeta_{m1} \\ -\zeta_{02} & \zeta_{m2} & \zeta_{02}\zeta_{m2} \\ -\zeta_{03} & \zeta_{m3} & \zeta_{03}\zeta_{m3} \end{bmatrix}, \qquad \mathbf{X} = \begin{bmatrix} A \\ B \\ C \end{bmatrix} \qquad (16)$$

Individual values for the unknown parameters can easily be found by Cramer's rule.
To increase the accuracy of the calibration procedure, more initial polarisations are required, by additional fitting procedure, based e.g. on Gauss-Newton algorithm that is simple and fast[9].

G. Application to the plasma measurements

In the case of the beam crossing a magnetised plasma, the initial polarisation ζ_0 is changed so that at the front of the optical detection system the beam has polarisation ζ_p. Then the final, measured polarisation state will be:

$$\zeta_m = \frac{1 + A\zeta_p}{B + C\zeta_p} \qquad (17)$$

Therefore, applying the calibration parameters A , B and C , it is possible to evaluate the polarisation state of the beam after crossing the magnetized plasma as:

$$\zeta_p = \frac{1 - B\zeta_m}{-A + C\zeta_m} \qquad (18)$$

From this one can easily recover the information on azimuth angle, ellipticity and phase shift and amplitude ratio with the following formulas[9]:

$$\begin{aligned} &\text{Azimuth angle} && \Psi = \mathrm{Re}(\arctan \zeta_p)] \\ &\text{Ellipticity} && \varepsilon = \tanh[\mathrm{Im}\,(\arctan \zeta_p)] \\ &\text{Phase shift} && \varphi = angle(\zeta_p) \\ &\text{Amplitude ratio} && \Theta = \arctan[absolute(\zeta_p)] \end{aligned} \qquad (19)$$

H. Evaluation of line-integrated measurements

In the case of JET, at least for the vertical channels, the major constribution of the magnetic field component perpendicular to the laser beam direction is the toroidal magnetic field, approximatively constant along the path. The equation (3) simplifies to:

$$LID_{polarimetry} = \int n_e\, dz \approx CONST \times \frac{\Phi}{\lambda^3 B_T^2} \qquad (20)$$

Here λ is the laser wavelength n_e is the plasma density B_T is the toroidal magnetic field in the core and *CONST* is a constant depending on the channel geometrical position within JET vacuum vessel centre.

The discrepancy between the line-integrated density measured by polarimetry with respect to interferometry can be explained by the mutual interference between Faraday Rotation and Cotton-Mouton effects[13,14] as well as the fact that perpendicular component of the total magnetic field is not exactly the toroidal field

To alleviate the first effect, at least in the JET case, we decided to use the LID derived from ellipticity as will be explained in the following section.

The relationship between ellipticity, defined as $\varepsilon = \tan\chi$ and azimuth Ψ and phase shift angle $\varphi = \Phi$ (as $\varphi_0 = 0$) is as follows:

$$\tan\Phi = \frac{\tan 2\chi}{\sin 2\Psi} \;\; or \;\; \tan 2\chi = \sin 2\Psi \times \tan\Phi \qquad (21)$$

As can be noticed the initial setup of 45 degree for azimuth angle maximises[3] the ellipticity.

Before the plasma pulse, equation (21) therefore becomes:

$$\tan\Phi = \frac{\tan 2\chi}{\sin 90} = \tan 2\chi \qquad (22)$$

In the small Faraday Angle approximation, the Cotton-Mouton angle can be measured at any magnitude as:

$$\tan\Phi \cong \tan 2\chi \qquad (23)$$

However, at larger Faraday Rotation and Cotton-Mouton angle this dependence becomes more important and above equation is not anymore valid as the Faraday angle component in equation (21) is not negligible anymore.

On typical JET plasma with high current and high density the Faraday Rotation and Cotton Mouton angle are larger than 10 degrees even at small ellipticity (χ<<5degrees).

Just as a simple mathematical exercise, for an angle variation of 15 degrees (from the initial value of 45 deg) equation (21) becomes:

$$\tan\Phi = \frac{\tan 2\chi}{\sin(2\times[45-15])} = 1.15\times\tan 2\chi \qquad (24)$$

As the LID varies linearly with Cotton-Mouton angle, the impact of this mutual interference on density is relevant (>10% in this example).

To resolve the mutual interaction between the two effects one has to use a complicated mathematical apparatus of a set of self-consistent differential equations for which the solution can be found only if both density and current profiles are known a priori (see ref 3). This is not the case for the on-line real-time calibration.

Therefore, in the JET case, for the core channel it was found empirically and with the mathematical support described above, that instead of the expression in (20), a new formula for LID derived from polarimetry using ellipticity can be expressed as:

$$LID_{ellipticity} = \int n_e\, dz \approx CONST \times \frac{2\,\chi}{\lambda^3 B_T^2} \qquad (25)$$

With respect to the second reason of discrepancy between interferometry and polarimetry derived LID, due to the field structure(see figure 13 in section IV), this is an open problem as we do not have the magnetics structure in real-time yet (EFIT++ being an offline program and the real-time EQUINOX package was not designed for protection systems).

II. Measurements

A typical example of the calibration results is shown in figure 7.

Here, the top left pictures represent the real and imaginary part of ζ_m, were the bottom left display the calculated values of the phase shift and Faraday angle during the calibration period. For completeness, the Faraday rotation and Cotton-Mouton angle calculated with the CAR method during plasma pulse are also displayed on the right side of the figure.

The error level for both Faraday and Cotton-Mouton angles is 0.2 degrees or less.

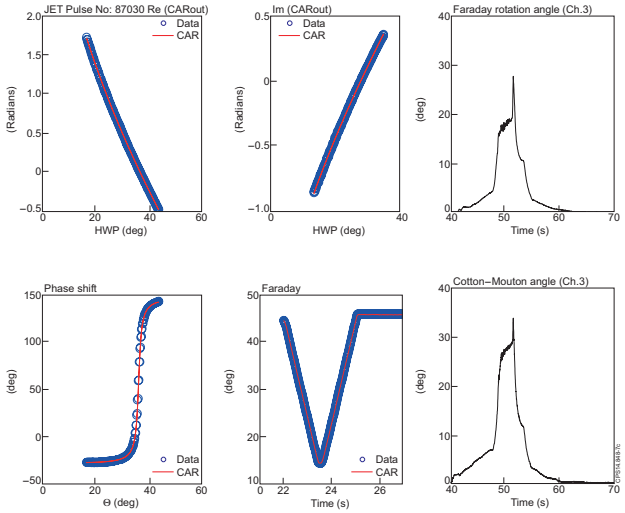

Figure 7 ζ_m calculated (line) and measured (circles) polarisation state, Faraday rotation angle and Cotton Mouton phase shift during the calibration period (22-32seconds) and during a JET plasma discharge (starting at 40 seconds).

On the following table are the values of the calibration parameters as well as the quality of the fit evaluated with the coefficient of determination[10].

Calibration parameters	Real part	Imaginary part
A	1.37983	-0.0406649
B	0.193856	0.0948332
C	0.259949	0.162677
Coefficient of Determination	0.999757	0.999960

Table 1: Example of calibration output for channel 3 on pulse 87030.

The measured range calibration parameters is dependent mostly on laser conditions. Figure 8 is an example of the evolution of the calibration parameters *A, B* and *C* for 100 consecutive pulses (one week of experimental campaign at JET). For this week, the parameter values are spread on a small bandwidth even for large variation of laser power during the operational day. It has been noticed that this has a small impact on Faraday Rotation angle measurements but it has some impact to the signal to noise ratio (SNR) of the evaluated density based on polarimetry and sometime the the error level in term of density is larger than one fringe.

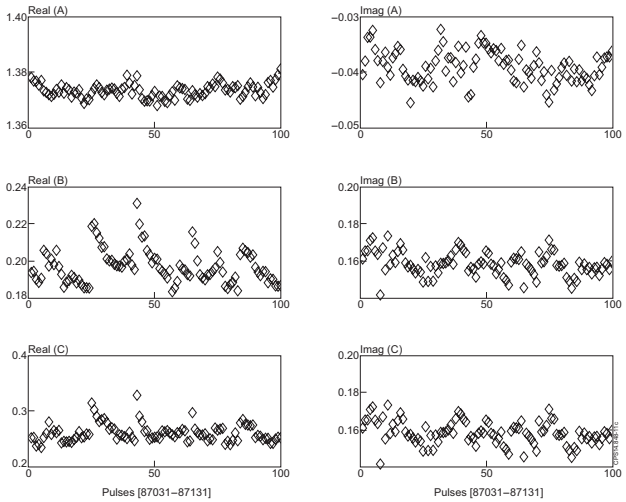

Figure 8. Evolution of calibration parameters for 100 consecutive plasma pulses during the 2014 JET campaign.

The new method is very robust even when the laser signal level is 30dB lower than nominal value and is operational on all eight channels as displayed in figure 9.

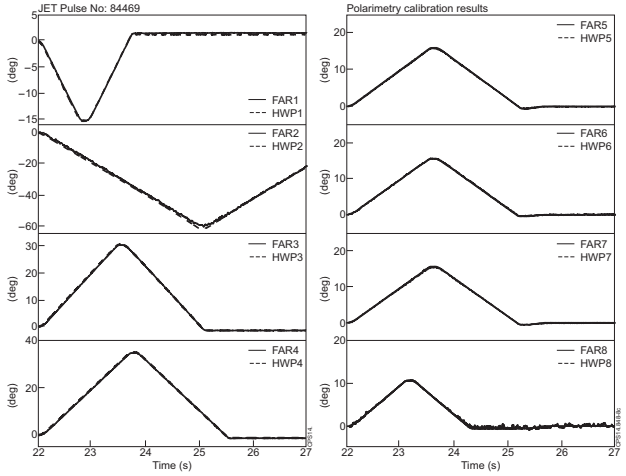

Figure 9. Calibration output for all 8 channels. HWP and FAR represent the mechanical position of the half-wave plate and the calculated Faraday Rotation angle from the detected laser signals.

The measurements of the new real-time system are very similar to the CAMAC-based counterpart but with better resolution due to the lower bit noise of the PowerPC system. An example of this comparison is given in figure 10 that contains the calculated Faraday rotation angle for the vertical channels for all recorded data including calibration time.

The method was tested extensively and with particular attention to high performance plasmas with high current during which the Faraday angle and Cotton Mouton phase shift are large (>15 degrees).

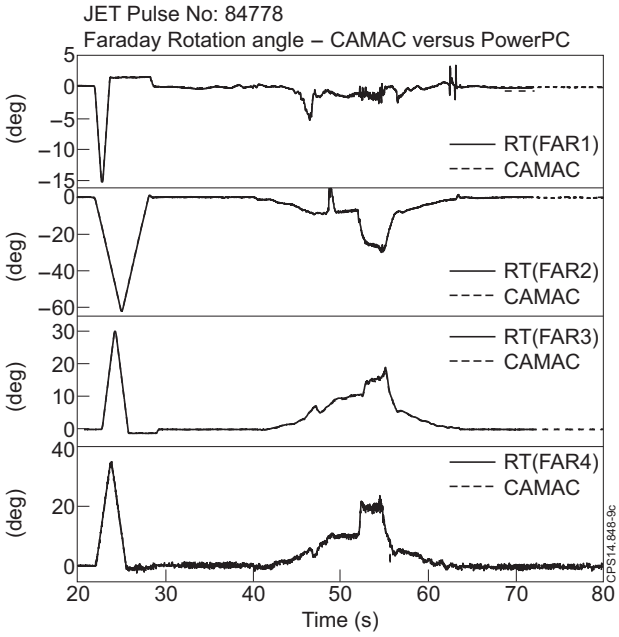

Figure 10. Measured Faraday rotation angles for the vertical channels during pulse 84778 – solid lines are measurements from the new PowerPC-based system and dashed lines from the old CAMAC-based system.

An example is displayed in figure 11 for a pulse with 3.5MA plasma current and more than 20MW additional heating power. In this pulse the maximum Faraday angle is greater than 20 degrees and the Cotton Mouton angle more than 30 degrees whilst the line-integrated density has a value of 20 fringes (1 fringe equals with 1.143×10^{19} particles/m^2).

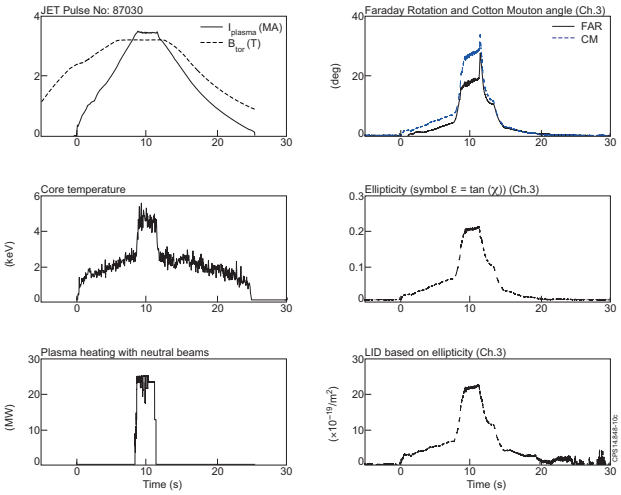

Figure 11. Various plasma parameters and polarimetry measurements for the high current plasma pulse 87030.

IV. INTEGRATION OF POLARIMETRY INTO MACHINE PROTECTION

A. Preamble

The current JET machine has measurements of the line-integrated density (LID) provided by interferometer, hard wired into the density feedback system and the interlock system of additional heating by neutral beams injection (NBI). With the installation of the new ITER-like metallic wall of the vacuum vessel, advanced plasma scenarios and new effects such as tungsten impurity influx into plasma, put the interferometer signal at risk. The interferometer's major weakness is that it is a history-dependent measurement (within the pulse) and any loss of signal for long enough time intervals will invalidate the measurement for the rest of the discharge. In the past, JET relied on a backup of density provided by Bremsstrahlung radiation measurements but in the ITER-like wall this measurement is deemed not safe for NBI protection due to potential contamination by tungsten line radiation.

After a detailed validation phase, JET now operates with the line-integrated density from polarimetry as a backup measurement to the one provided by interferometry. In figure 12 is depicted the flow-logic of the Plasma density validation (PDV) at JET. Every signal within PDV has an equivalent validity flag and the signals are activated in a cascade manner (Ranks). The logic is kept simple as it is very important that the signal provided to PDV to have a very stringent quality control and automatic validation implemented.

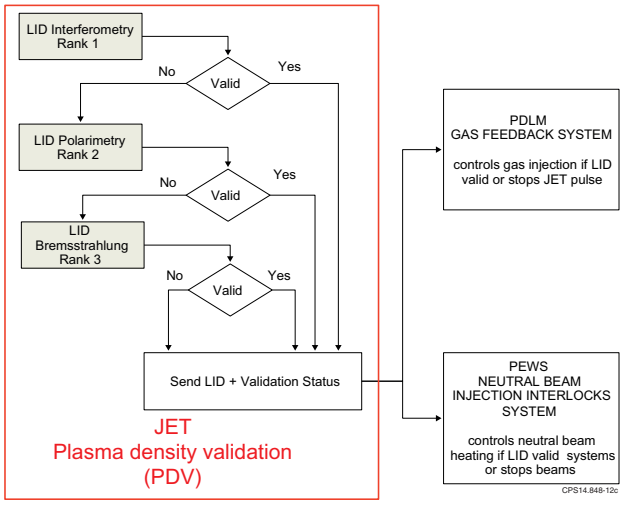

Figure 12 Plasma Density Validation (PDV) and links with various Protection Systems

The LID measurement from polarimetry has some limitations such as:

- Mutual interference between Faraday and Cotton-Mouton effect are very strong at high density
- 10ms delay in data provision due to the integration time of electronics
- The fact that in evaluating the density we ignore the impact of diamagnetic effects
- Radial and poloidal magnetic fields contribution to total magnetic field not readily available in real-time as to obtain this information one has to compute a very complex magnetic field structure software inversion.

An example of the reconstruction of LID from ellipticity using the approximation given in equation 25 is shown in figure 13. In this figure, the use of the vacuum toroidal magnetic field (PPF/MAGN/BVAC) is compared to evaluating equation 25 using *a posteriori* the toroidal field calculated from an equilibrium reconstruction for this discharge (EFIT++/B_t). One can see in the top left panel of figure 13 that the equilibrium toroidal field can vary by about 1% from the vacuum field. This can generate an error in the calculated LID of 2%. This is an important source of error at low density and low Faraday angle (bottom right panel of figure 13). During the high density phase (7-12 s in this example), on the other hand, the dominant error is due to the interaction between the Faraday rotation and the Cotton-Mouton effect. For the vertical line-of-sight shown in figure 13, the correction due to radial field is expected to be small as its magnitude is only about 2% of the toroidal field (bottom left panel of figure 13) and it enters via the Cotton-Mouton effect only as (B_t^2 - B_r^2) (equation 3). Corrections due to the vertical field (bottom left panel of figure 13) enter via the Faraday rotation (equation 2) and are expected to be small at low Faraday angles.

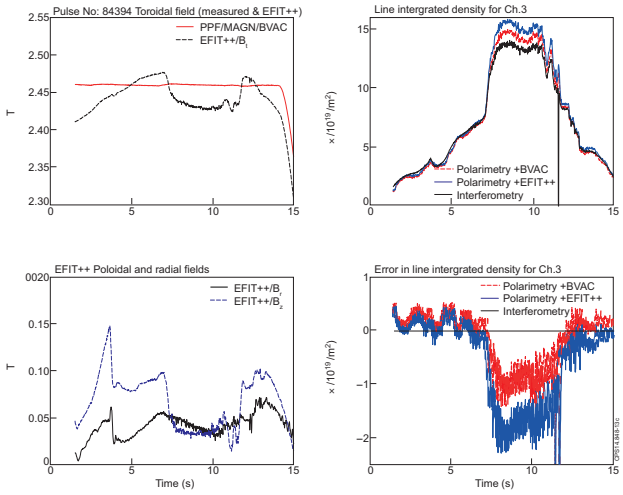

Figure 13 Line-integrated magnetic field components normal to propagation direction of channel 3 of polarimetry and calculated line integrated densities using ellipticity and toroidal field and EFIT components

It is worth mentioning that the original polarimeter design was on the assumption that there is no mutual interaction between Faraday Rotation and Cotton-Mouton effects. Recent studies shown this is not true and that the CAR technique can handle the coupling of the two effects[3,6].

We alleviated these effects by evaluating line-integrated electron density from ellipticity (see eq.25) and not Cotton-Mouton phase shift angle and by scaling (division) the measured density from polarimetry in order to ensure that the new measurement *always underestimates* the actual density (measured normally by the interferometer) by a certain value so polarimetry errors are the side of caution from the JET machine protection point of view. The implementation of the new measurements was following a

very strict set of rules and involved several software iterations and parallel checks. The current scaling factor has been set to the value 1.2 using a very conservative approach (ref.pulse 87030). The current value range will be revised based on experience that will be acquired in the next campaigns.

The new method of calibration proved to be very robust for the JET configuration even if the system is not optimised for the best signal to noise ratio. However it was observed that the laser power has a strong impact on the line-integrated electron density measurements from polarimetry as the error level in this case can be larger than one fringe. This becomes critical when this measurement is used actively for plasma gas feedback control and protection systems so further instrumentation is being added to monitor better the lasers.

Figure 14 shows a typical example of the evolution of the density control in the case of a pulse with a tungsten impurity influx. In this particular case the control of density switched to one of the interferometer lateral channels after the main vertical channel of interferometry fails as early as about 10.4s from plasma start (signal level for core drops to zero, third plot from the top). One can notice that the LID provided by the polarimeter is stable for the entire length of the pulse (validation error flag remains zero for the entire length of the pulse)

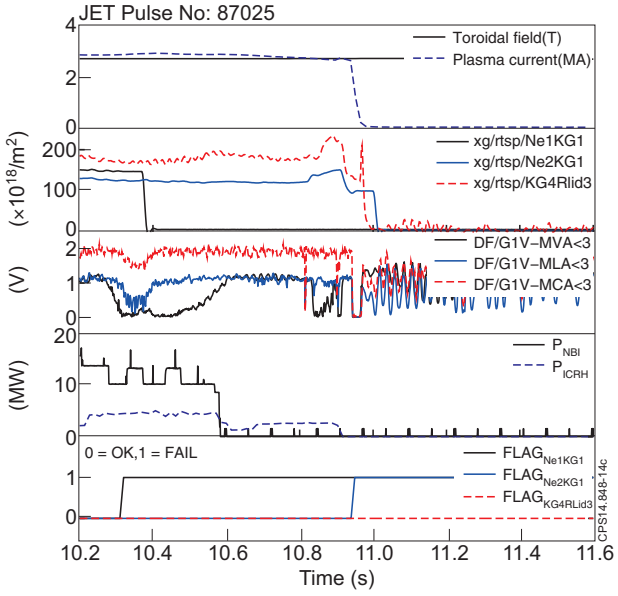

Figure 14. Example of various line-integrated density (LID) measurements used for machine protection at JET (Ne1/KG1, Ne2/KG1, KG4Rlid3 are LID for channels 3 and 7 from interferometry and channel 3 from polarimetry, respectively); G1V-MVA<3 and G1V-MLA<3, are the signal levels of DCN lasers for channel 3 and channel 7, respectively; and G1C-MCA<3 is the signal level for methanol laser for channel 7.

A similar example is given in Figure 15 where one can also notice that the plasma is heavily affected by these tungsten impurity events and level of radiation is very high. The LID from interferometry was reconstructed offline but there is a time interval when the density was deemed not valid and was set to zero.

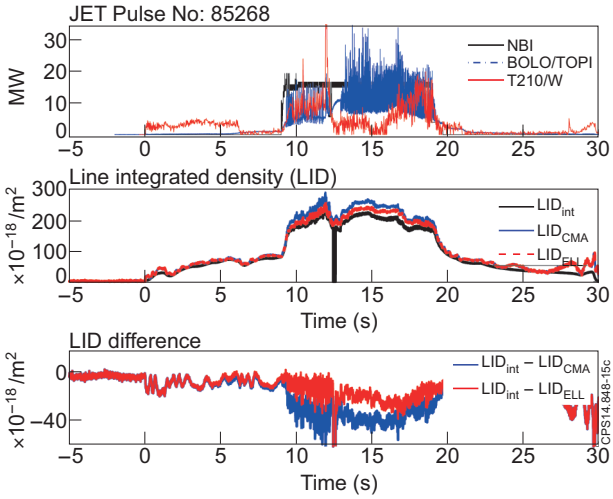

Figure 15. Line-integrated density for a pulse that is affected by tungsten impurity influx (NBI is the total Neutral Beam power, BOLO/TOPI is the level of radiation, and T2IO/W represents the tungsten level as detected by JET KT2 spectrometer diagnostic)

Another point shown by this picture that can be noticed is the quantitative discrepancy between LID derived from ellipticity and Cotton-Mouton angle with respect to interferometry (third plot). As the difference between the LID from interferometry and polarimetry is larger for plasmas with high Neutral Beam Power (NBI) (>15MW), high plasma currents and high magnetic field, several statistical analysis were done to get a better estimation of the density in the view of use for machine protection and control. One such example is displayed in figure 16 for an entire experimental session (13 pulses). One can notice a LID difference of around 10% that does not depend of the magnitude of additional heating power. The reason for this difference can be partially explained by the fact that the formula evaluating the line-integrated density from polarimetry does not include the radial and poloidal components of the total magnetic field as shown in figure 13. There is also a second order correction required due to the mutual interaction of the Faraday rotation angle and Cotton Mouton phase shift angle not fully mitigated by the use of the ellipticity in evaluating the LID. In this particular case a calibration factor of 1.2 (division of LID from polarimetry by 1.2) will bring this measurements on the safe side for use for machine protection that requires that the difference between measurements has to be in the range of 3 fringes (~30x10^{18}/m^2)

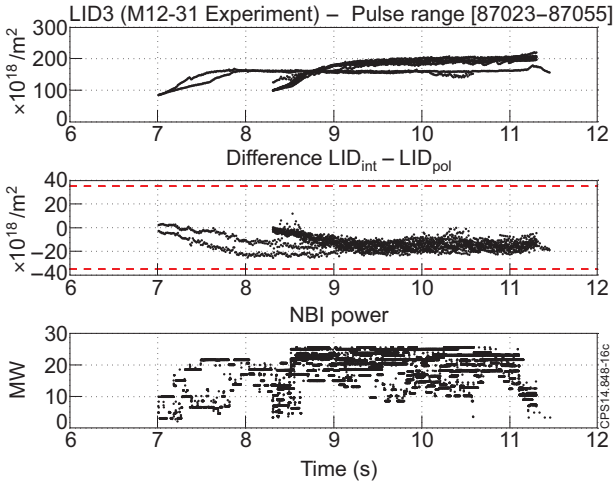

Fig 16 Time evolution of the line-integrated density difference between interferometry and polarimetry for pulses form an entire experimental session.

The JET machine is a nuclear facility and any change of control requires extensive testing and fault simulation. Many offline tests were done by injecting previously recorded analogue data into the real-time crate PowerPC to simulate fault conditions and validation flag analysis. Following these tests, in August 2014 the Machine Protection Working Group approved the use of the LID signal from polarimetry for real time control of both gas feedback and machine protection systems (NBI interlock).

This is the first time in the world that polarimetry has been used unattended for plasma control and protection of the machine (the Faraday Rotation measurements are normally used in real-time control for q-profile in advanced scenarios but with strong interaction from a specialist).

This measurement proved to be 100% reliable from the first day.

In figure 17 is such an example. In this pulse, with low plasma density, there was an injection of 3mm diameter pellets that penetrated the core causing a density increase of 80% in a few milliseconds.

The top figure pictures the following four LIDs: the gas feedback control(*xg/rtsp/pdlmLid*), the NBI protection density (*xt/rtsp/pewsLid*), interferometry(*xg/rtsp/ne1Kg1*) and polarimetry(*xg/rtsp/KG4Rlid3*).

The current interferometry implementation for LID detects a fault(validation flag *JPF/XG/RTSP/STA1KG*1 becomes negative in second figure) and the PDV switches safely to polarimetry LID is still valid (the corresponding flag *XG/RTSP/KG4RLID3/D* stays positive) and carries on for the rest of the pulse..

The difference between interferometry and polarimetry LID is below the limit of 20 x10^{18}/m^2 as displayed in the fourth plot.

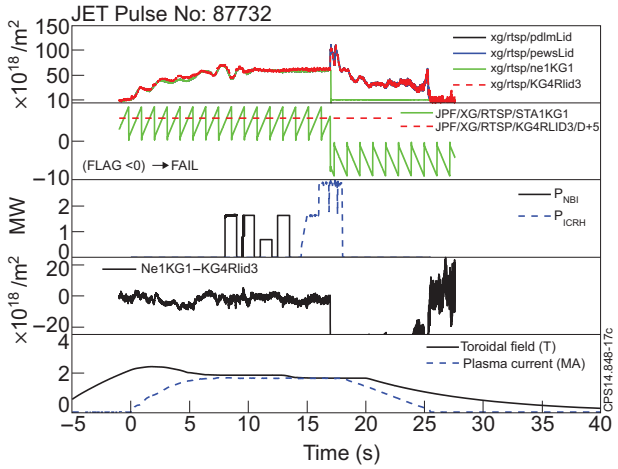

Figure 17 Example of a pulse when LID from polarimetry was actively used for controlling gas feedback control and NBI protection on a JET plasma (top figure displays various LIDs used for machine protection and gas feedback control, figure two the validation flags for interferometry and polarimetry respectively, third plot displays NBI and ICRH power and bottom plot the main parameters of toroidal field and plasma current)

V. CONCLUSIONS

A fast and reliable automatic polarimetry calibration based on the Complex Amplitude Ratio method has been implemented at JET in order to provide measurements of Faraday rotation angle and line-integrated density measurements in real-time with one millisecond time resolution. The new measurements are integrated with the new offline magnetic reconstruction code EFIT++ but more important, the measurements of the LID from polarimetry are also integrated with JET plasma control and machine protection systems.

The polarimeter, with this new addition, will become an essential diagnostic for the JET experiment for the following campaign and in particular the D-T campaign which is a very important step for ITER developments.

This new diagnostic implementation is expected to have a great impact not only on the design of the new polarimeters envisaged for other machines (ITER, JT60SA for example) but also on their application as this type of diagnostic could acquire elevated importance for density control and as a safety feature for plasma experiments.

V. FURTHER DEVELOPMENTS

We are envisaging new developments in several areas: data acquisition hardware upgrade (CPU upgrade), better magnetic structure information to the polarimeter (radial field information for example), a new design of the half-wave plate assembly that can be removed/serviced via remote-handling (essential during D-T operation).

VI. ACKNOWLEDGMENTS

We would like to thank to all our colleagues at CCFE and EU associations for this work, in particular to M.Kempenaars and F.Orsitto for careful reading and suggestions but also to A.Murari, E.Zilli, M.Brombin, M.Gelfusa, P.Gaudio, M.Maslov and S.Dudley for previous work they have done in this field over recent years.

This work has been carried out within the framework of the Contract for the Operation of the JET Facilities and has received funding from the European Union's Horizon 2020 research and innovation programme. The views and opinions expressed herein do not necessarily reflect those of the European Commission.

References:

[1] A Boboc *et al*, Rev. Sci. Instrum.**77**, 10F324 (2006)
[2]Segre, Plasma Phys. Controlled Fusion **41**, R57 (1999)
[3] K. Guenther and JET-EFDA Contributors, Plasma Phys. Controlled Fusion **46**, 1423 (2004).
[4] B. Alper *et al,* 37th EPS Conference, P2.173,2010, to be published
[5] A Boboc *et al*, IRMMW-THz. Conference, Vol. 1, p 378-380 (2007)
[6] M. Gelfusa *et al*, Rev. Sci. Instrum. **81**, 053507 (2010)
[7] F P Orsitto *et al*, Plasma Phys Contr Fus 50 (2008)
[8] I Scierski and F Ratajczyk, Optik **68**, 121 (1984)
[9] B Bieg *et al*, Fus. Eng. Design **88**, 1452 (2013)
[10]http://en.wikipedia.org/wiki/Coefficient_of_determination
[11] Mazon D. *et al*., Plasma Physics and Controlled Fusion. 45:L47-L54(2003)
[12] L. C. Appel *et al*, "A unified approach to equilibrium reconstruction," in 33rd EPS Conference on Plasma Physics (Rome, Italy, 2006), P-2.184.
[13] F P Orsitto et al. Rev Sci Instr 81(2010)10D533
[14]S. E. Segre, Plasma Phys. Controlled Fusion 35, 1261 1993
[**] full documentation of CODAS electronics is managed through internal JET Document Notes (JDN) documentation that is not freely available but could be provided on request